

# Spatially resolved detection of miniaturized reaction–diffusion experiments in chip reactors for educational purposes

T. Kirner<sup>a,\*</sup>, P. Jaschinsky<sup>b</sup>, J.M. Köhler<sup>a</sup>

<sup>a</sup> Department of Physical Chemistry and Microreaction Technology, Institute of Physics, Technical University of Ilmenau, Weimarer Str. 32, D-98693 Ilmenau, Germany

<sup>b</sup> Department of Technical Physics I, Institute of Physics, Technical University of Ilmenau, Weimarer Str. 32, D-98693 Ilmenau, Germany

## Abstract

A reactor consisting of plastic foils was developed for educational purposes. The reactor works with small volumes and can be operated at continuous flow conditions. In practical courses for undergraduate students of engineering, the reactor was used for simple diffusion and reaction–diffusion experiments. In the initial experiments, the diffusion coefficient of malachite green in different viscous liquids was estimated. The dependency of the diffusion coefficient on the viscosity of the solvent by using water and 30% glycerol could be reproduced by the students. In the subsequent experiments the generation of iron rhodanide from iron chloride was chosen as a simple test experiment for reaction–diffusion systems. The experiments with iron rhodanide showed the dependency of the spreading fronts on flow conditions. © 2003 Published by Elsevier B.V.

*Keywords:* Reaction–diffusion systems; Intensity profiles; Microchannel

## 1. Introduction

Methodical differences as well as difficulties in handling, and in particular the low importance of chip reactoric variants in education, represent a substantial barrier for the rapid development, maturing and use of microtechniques in chemistry. Therefore, it is necessary to develop environmentally compatible and resources conserving chemical working by miniaturization [1], not only for technical development and production but also in research and education. In the first place, such experiments were chosen as examples that are suitable for fast experimentation. The intention was to miniaturize and test exemplarily experiments, in the low microliter range. While developing appropriate experiments, we focused on simple feasibility rather than on scientific originality. The intention was to get simple chemical and physicochemical statements, respectively, within a few hours. In addition, the instrumental side of microreaction technology should be demonstrated as substantial characteristic of miniaturized material operations and their control. With this procedure the goal was pursued to connect research work directly with educational activities.

For the experiments, liquid-phase reactions and physicochemical measuring processes were selected. Preferably, the

reactions should be performed in small reaction vessels or in drops stationarily or in microchannel arrangements in a continuous flow. The procedures should run off fast enough and be comprehensible by simple, preferably optical spectroscopical measurements. As a device for visual control and optical measurements simple microscopes should be applicable. In contrast to microsystem engineering, a multilayer foil reactor was developed. This reactor was used for student experiments.

The reactor was applied within a basic practical course in chemistry to determine the diffusion coefficients of a dye assigned in differently viscous liquids. In addition, the experiments were extended on simple reaction–diffusion systems with and without additional flow. Besides making the students come into contact with basic principles of microreaction technology, the other educational aims were to give them knowledge about transport phenomena by the example of diffusion and reaction–diffusion systems with and without convection and with different viscosities. An additional effort in these experiments was to introduce photometric measurements and the Lambert–Beers law [2,3].

## 2. Experimental

The core piece of the experimental setup is the flow reactor. The reactor works with a volume in the range of 100  $\mu$ l.

\* Corresponding author.

E-mail address: thomas.kirner@web.de (T. Kirner).

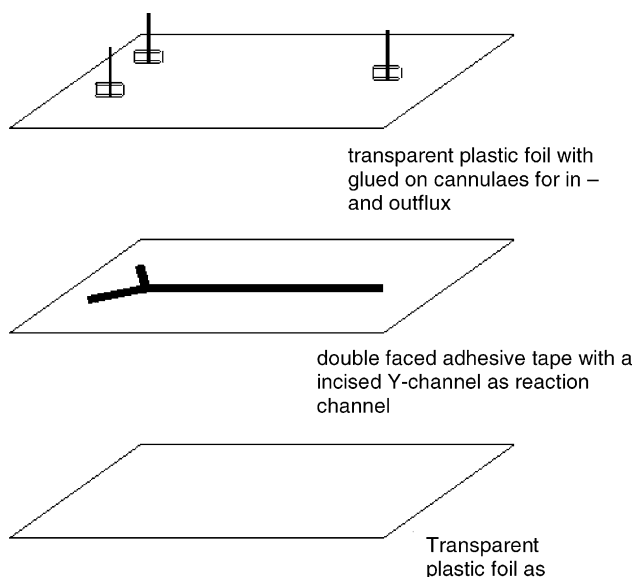


Fig. 1. Sketch of the microflow reactor consisting of three layers.

As in microreaction engineering [4–6] the reactor was made of multilayers (Fig. 1), actually three layers in this case. The bottom layer is just a plastic foil (as used for overheads). On this layer a double-faced adhesive tape (Tesa, Germany) was fixed. This includes the structure of the reaction channel and the two influx channels. These channels were cut with a scalpel in the adhesive tape. No master was used. The structure was drawn simply on the protection film of the tape with a marker. After cutting the structure into the tape it was fixed to the bottom layer. Then the remaining protection film was removed and the top layer fixed on it. This layer is also just a piece of plastic foil. In this foil holes were pierced for in- and outlet. Small parts of silicon tubes (inner diameter: 0.5 mm, wall thickness: 1.0 mm; Roth, Germany) were used for stabilizing the cannulae (outer diameter: 0.6 mm; Roth, Germany) which are glued (Uhu® Plus Schnellfest, Germany) on to the foil over the holes.

The widths of the channels were between 0.5 and 1 cm. The thickness of the tape that means the depth of the channel was 0.3 mm and the length was chosen between 1 and 4 cm. Two plastic syringes (1 ml; Roth, Germany) driven by a syringe pump (SP210iw; World Precision Instruments

Inc., USA) were used for loading the reactor with reactants (Fig. 2). The connection between the reactor and the syringes was done by a connecting tube (polyethylene, inner diameter: 0.4 mm, outer diameter: 0.8 mm; NeoLab, Germany) or PTFE (inner diameter: 0.3 mm, outer diameter: 0.76; Novodirect, Germany) and cannulae were fixed with two components glue (Uhu® Plus Schnellfest, Germany). For better contrast, a filter (BG12; Linos AG, Germany) was used (not shown in the sketch) which was laid simply on the reactor and a blue glass filter was added in the optical path between light source and reactor. The two filters were not used in each experiment. The light source was placed below the reactor and transmitted light was detected by a video microscope (Motic DM143, Motic B1 series; VWR International, Germany).

### 3. Results

#### 3.1. Diffusion of malachite green

The diffusion coefficient of malachite green in water and in 30% glycerol solution, respectively, was determined. Malachite green in solvent (1 mg/1 ml water or 30% glycerol) was taken in one syringe and distilled water or 30% glycerol in water in the other syringe. The liquids were pumped into the reactor in order to introduce a step profile. After building up this profile, pumping was stopped and the reactor closed at the outlet with a clamp. The diffusing front of the dye was observed (Fig. 3). In this experiment we used the video binocular of Motic B1; a blue glass filter was added in the optical path between light source and reactor but no additional filter between reactor and detector. The measured variable is the transmittance  $T$ . To get a factor which is proportional to the concentration we calculated the absorbance  $E$  with  $E = -\log T$ .  $T$  was calculated from the images according to the following equation:

$$T = \frac{I_D}{I_0} = \frac{I_n - I_{\min}}{I_{\max} - I_{\min}} \quad (1)$$

where  $I_n$  is the value of the intensity measured with the CCD camera of the microscope and  $I_{\min}$  and  $I_{\max}$  the minimum and maximum values of intensity in the image, respectively.

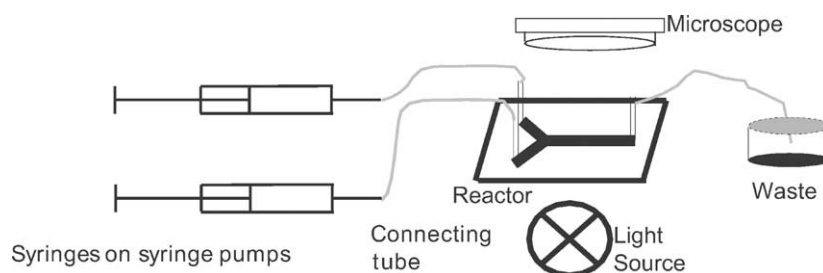


Fig. 2. Sketch of the experimental setup.

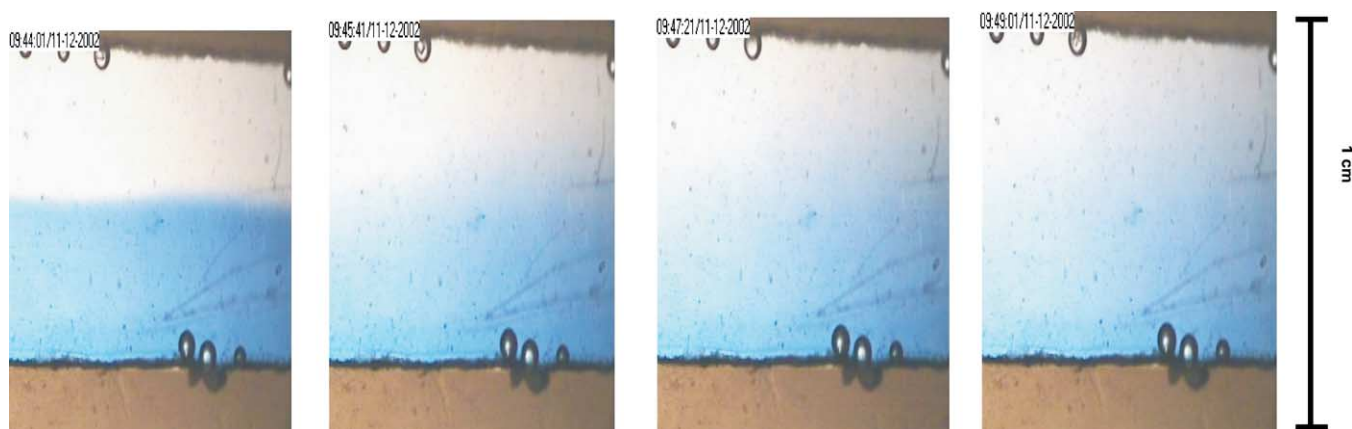


Fig. 3. Diffusing front of malachite green in water. The four images are examples of the time series which shows the spreading diffusion front. The numbers represent the time in seconds.

For evaluation rectangles of the images of the reactor channel are cut (Paintshop Pro, Jasc, USA), whose height corresponds to the channel width and whose width should be maximum. This depends on the initial profile. These rectangles were divided again into smaller rectangles. The widths of these rectangles were the same as in the bigger rectangles. The height would be ideally one pixel in the images. The students cut the rectangles to about 10 pieces. The average intensity of each of these smaller rectangles was calculated using the histogram function of the software. The averaged intensity is correlated to a space dimension  $x$ . The intensities were corrected with the maximum and minimum intensity of the image (Eq. (1)). The values of transmittance were converted to the absorbance and plotted against the distance of the rectangles. This gives the intensity profiles in Figs. 4, 7 and 9. To calculate the diffusion coefficient  $D$  of this profiles, the Einstein–Smoluchowski equation,  $D = \Delta x^2 / 2t$  [7], was used. Thereby  $x$  represents the distance of diffusion and  $t$  the time.  $x$  and  $t$  are determined by averaged absorbance profiles of the images. As shown in Fig. 4, the distance  $\Delta x$  was obtained by tangents on the inflection points of the curves.

The students transformed about 10 images of a time series into intensity profiles. The differences of the intersection of these tangents to the space axis  $x$  of two tangents represent in each case the distance of diffusion. To each of the profile a time is associated. With the time differences and the diffusion distances for about 10 couples of profiles, a constant  $D$  was calculated using the Einstein–Smoluchowski equation. The average value was taken as diffusion coefficient. With these distances and the corresponding time, we obtained for the images in Fig. 2 a diffusion coefficient of  $D \approx 2.6 \times 10^{-4} \text{ cm}^2/\text{s}$ . Twelve groups of undergraduate students carried out the experiments with malachite green solution in water and in 30% glycerol. The mean values of the diffusion coefficient found by the students are  $D = 4 \times 10^{-4} \text{ cm}^2/\text{s}$  for water and  $D = 6 \times 10^{-5} \text{ cm}^2/\text{s}$  for 30% glycerol. The values vary in water between  $D = 1.6 \times 10^{-3}$  and  $5.3 \times 10^{-5} \text{ cm}^2/\text{s}$  with a standard deviation of  $6 \times 10^{-4} \text{ cm}^2/\text{s}$ . In glycerol a standard deviation of  $1 \times 10^{-4} \text{ cm}^2/\text{s}$  with values which vary between  $3 \times 10^{-4}$  and  $6 \times 10^{-7} \text{ cm}^2/\text{s}$ . Despite the high differences in individual values, all groups found higher  $D$  in solutions of lower viscosity, as expected.

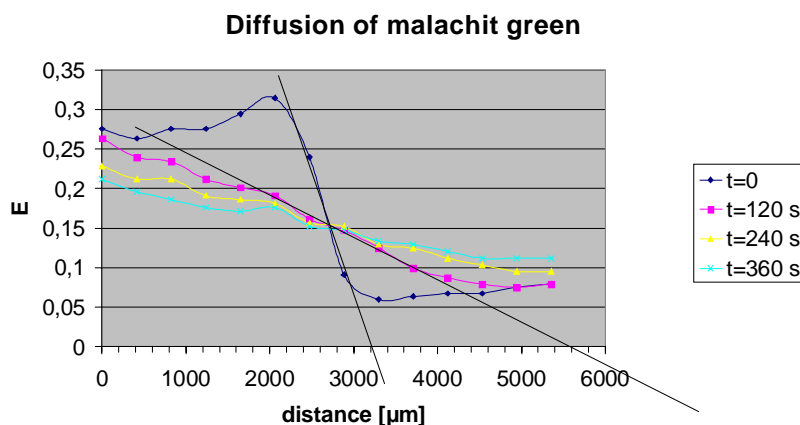


Fig. 4. Absorbance profiles of the images in Fig. 3.

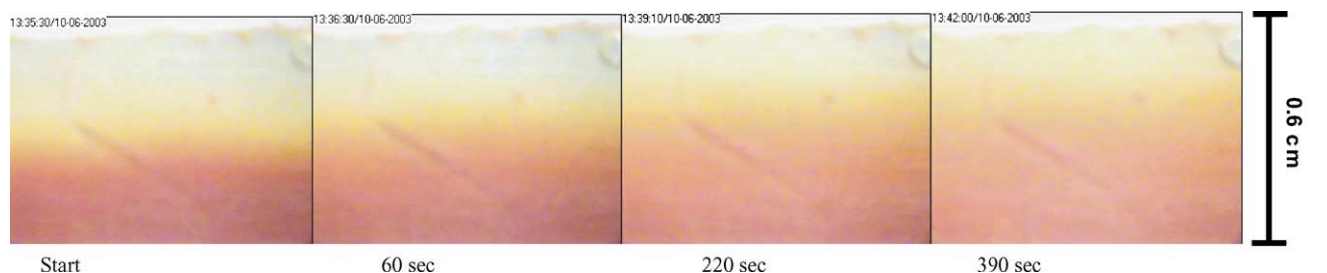


Fig. 5. Diffusion of iron rhodanide in water. The four images are examples of the time series. The numbers represent the time in seconds. In this experiment no filters were applied.

### 3.2. Diffusion of iron rhodanide

To determine the diffusion coefficient of iron rhodanide, the solution was premixed by adding 0.1 M  $\text{NH}_4\text{SCN}$  and 0.1 M  $\text{FeCl}_3$  into a reaction vessel. This results in an intense red-colored solution. The intense red color is due to different complexes of iron rhodanide with water [8]. This solution was pumped through one channel and distilled water through the other. For detection, a video stereomicroscope (Motic, DM143) was used (Fig. 5). Besides this, the experiment was performed as described in Section 3.1. The diffusion coefficient was determined again with the Einstein–Smoluchovsky equation for this series of images to be  $D = 4.2 \times 10^{-5} \text{ cm}^2/\text{s}$ .

### 3.3. Formation and diffusion of iron rhodanide

The reactant solutions were pumped into a foil reactor with a Y-shaped channel. The reaction proceeds in the interdiffusion zone of the two liquids (Fig. 6). The spreading of the reaction–diffusion fronts was observed with a video microscope (Motic, DM143), in subject to the flow rate. Different concentrations and flow rates were investigated. The red color of the product was observed.

Absorbance profiles of this time series were calculated additionally to the student's analysis (Fig. 7). The profiles were obtained by using the blue channel of the RGB image. This channel was converted into a list of numbers (Mathematica, Wolfram Research, USA). Lateral to the diffusion front the array was averaged. The obtained absorbance–distance plot was smoothed with a Savitzky–Golay filter of fourth order. In the experiment described above (Figs. 6 and 7) the diffu-

sion coefficient was estimated to be  $D = 3.3 \times 10^{-5} \text{ cm}^2/\text{s}$ . In Fig. 7 a small asymmetry is evident. This should be due to an additional convection. This convection is very small and probably due to incompletely clamped in- and outflow.

### 3.4. Reaction and diffusion of iron rhodanide with flow

To investigate the influence of additional flow on the system, the students investigated two different flow rates.

For these experiments some student groups used the stereomicroscope (Motic, DM143) and others the binocular (Motic, B1 series). In most experiments the blue filter (BG 12) between the reactor and the detector was used. The example image was taken with this filter and the stereomicroscope. The absorbance profiles were determined as described above (Fig. 9).

At a flow rate of  $10 \mu\text{l}/\text{min}$  the students still detected a spreading front (Figs. 8 and 9). Since the flow is lateral to the spreading reaction–diffusion front the contribution of reaction and diffusion is still higher than that of convection. The experiment with a flow rate of  $50 \mu\text{l}/\text{min}$  (Fig. 10) was done in the same way and with the same equipment. These experiments clearly show that the flux is high enough to lead to a stationary state after a short time. The reaction was kept in a small region of the interdiffusion of the two solutions  $\text{NH}_4\text{Cl}$  and  $\text{FeCl}_3$ .

## 4. Results and discussion

By diffusion one understands about the migration of particles toward a density gradient. It is described by Fick's

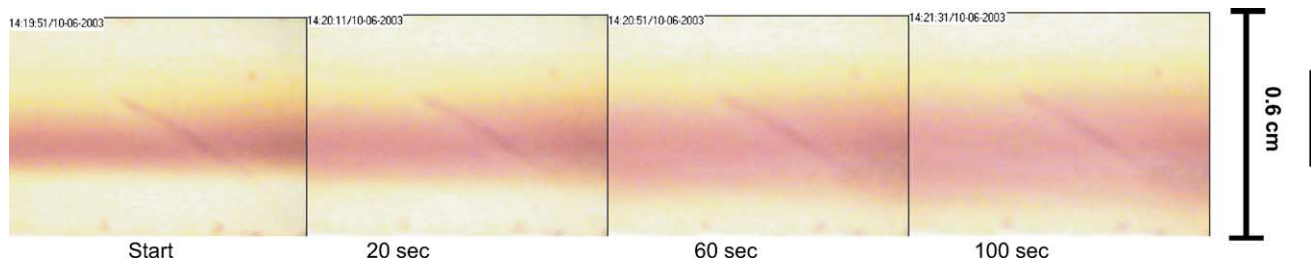


Fig. 6. Example images of the time series of in situ forming iron rhodanide. The numbers represent the time in seconds. The reaction proceeds at the interface of the two liquids.

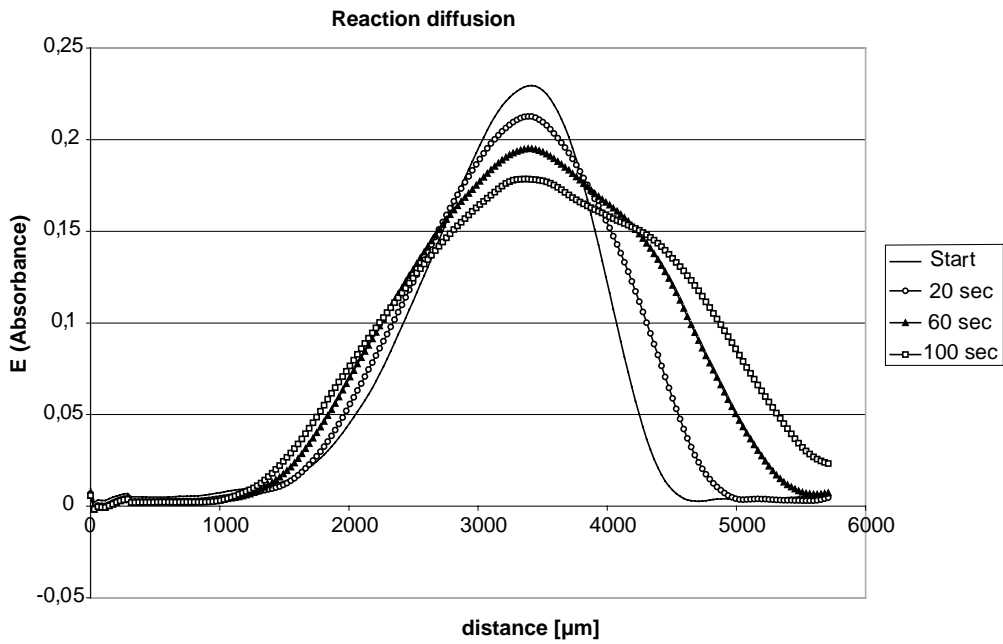


Fig. 7. Absorbance profiles of the example images of the time series in Fig. 6.

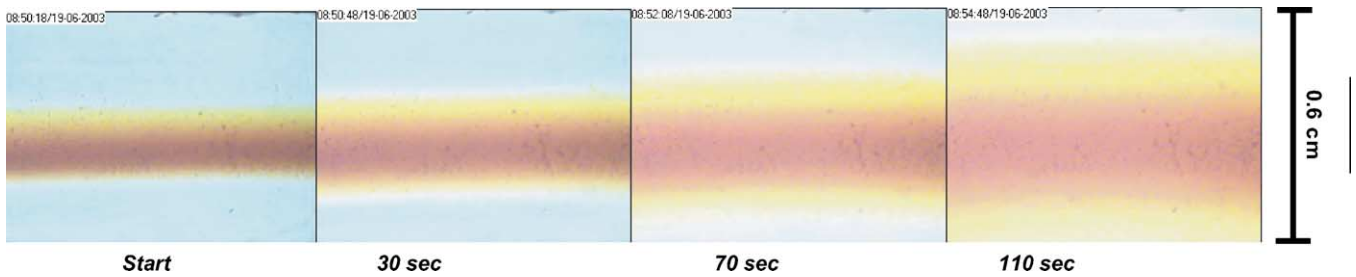


Fig. 8. Example images of a time series with in situ forming iron rhodanide at a flow rate of 10 μl/min. The numbers represents the time in seconds. The reaction proceeds at the interface of the two liquids. The spreading of the reaction–diffusion fronts was observed with a video microscope.

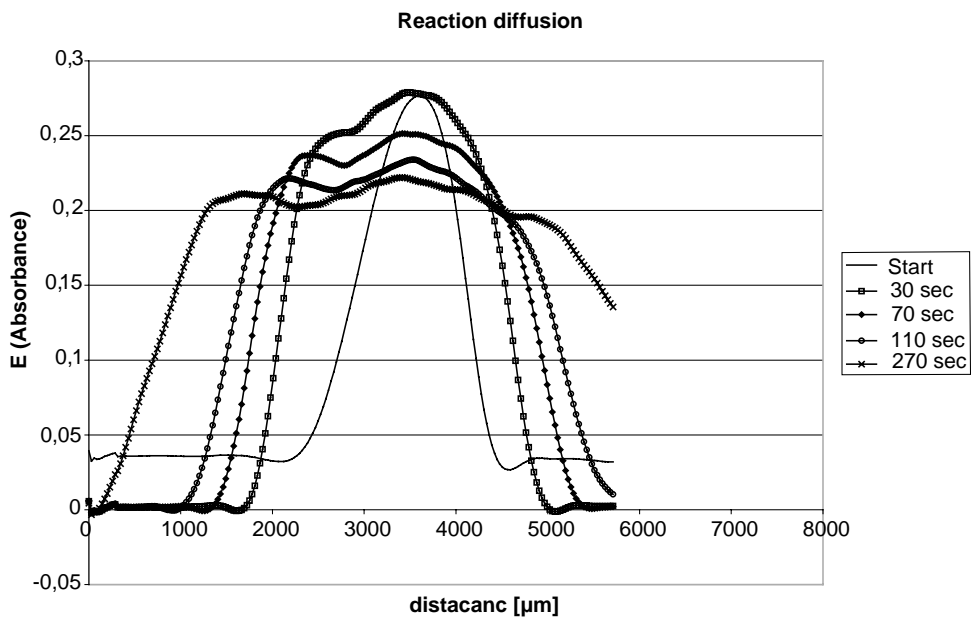


Fig. 9. The absorbance profiles were calculated as in Fig. 7. The profiles additionally show the image after 270 s.

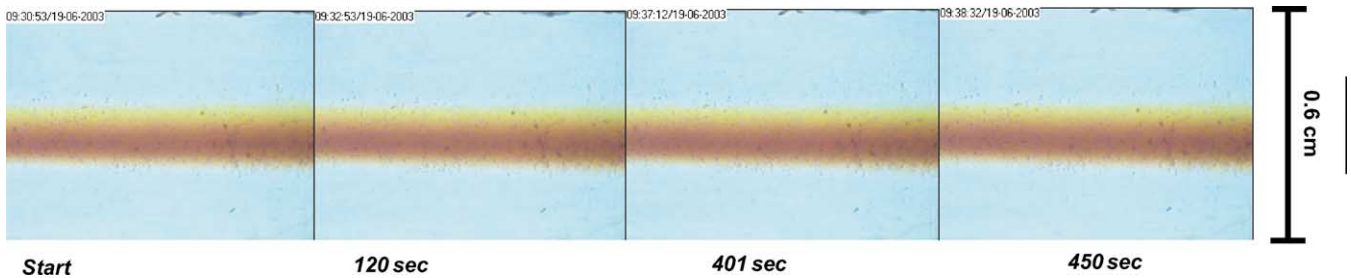


Fig. 10. Example images of a time series with in situ forming iron rhodanide at a flow rate of 50 µl/min. The numbers represent the time in seconds. The reaction proceeds at the interface of the two liquids. The front is not spreading.

laws. The first Fick's law of diffusion means that the particle stream is proportional to the density gradient:

$$J = -D \frac{dN}{dx} \quad (2)$$

The flow  $J$  corresponds to the number of molecules per surface and time unit,  $N$  is the particle density at the regarded place and  $x$  indicates the direction. The constant  $D$ , the diffusion coefficient, is a characteristic size of the diffusing substance, the medium and its characteristics (e.g. temperature).

If we consider changes of concentration within an inhomogenous range, we have to use the diffusion equation (second Fick's law):

$$\frac{\partial N}{\partial t} = D \frac{\partial^2 N}{\partial x^2} \quad (3)$$

This law describes the changes of particle densities (or concentrations) in an infinitesimal volume element by diffusion in and out to this volume element. This is a second-order differential equation, whose solution depends on the special experimental conditions. A detailed discussion with boundary conditions suitable to the experiments in this article is given for example in Ref. [9]. One solution of Eq. (3) for special boundary conditions (at  $t = 0$  all particles  $N_0$  are in the  $yz$ -plane (with the surface  $A$ ) with  $x = 0$ , the concentration is everywhere finite and all  $N_0$  particles are present at all time) is

$$N = \left[ \frac{N_0}{A(\pi Dt)^{1/2}} \right] e^{-x^2/4Dt} \quad (4)$$

Thus, the concentration of the particles at any point can be computed. The root mean square distance traveled by diffusing particles in a certain time under the applied conditions is

$$\bar{x} = \left[ \int_0^\infty \frac{x^2 NA}{N_0} dx \right]^{1/2} = (2Dt)^{1/2} \quad (5)$$

The diffusion coefficient  $D$  is represented by  $D = x^2/2t$ . In fact this equation was used for determining the diffusion constant. If one considers diffusion from statistic view as a process being based on random particle movements and thereby overcomes a particle in time  $t$  at distance  $x$ , then

one receives the Einstein–Smoluchowski equation (see, for example, Ref. [3])

$$D = \frac{x^2}{2t} \quad (6)$$

This equation is the link between the microscopic details of the particle movement and the macroscopic parameters of diffusion. Strictly speaking, in the statistic view  $x$  is not identical to the  $x$  above (Eq. (5)). Here it represents the step length of the jump of an individual particle and  $t$  is here the rate at which the jump occurs. The connection of the microscopic basic principle of diffusion, the Brownian molecular movement and thus the statistic view with the Einstein–Smoluchowski equation, to the macroscopic diffusion equation was explained to the students. However, with the students in the basic course this topic was not continued to deepen.

Diffusion by substances in combination to reactions is described in the three-dimensional case by the following reaction–diffusion equation:

$$\frac{\partial \vec{c}}{\partial t} = f(\vec{c}) + D \left( \frac{\partial^2 c}{\partial x^2} + \frac{\partial^2 c}{\partial y^2} + \frac{\partial^2 c}{\partial z^2} \right) \quad (7)$$

whereby  $\vec{c}$  is the vector of the concentrations and  $f(\vec{c})$  corresponds to the reaction part.

In the experiments in this article the equation can be simplified to one-space dimension. If also convection has to be considered the equation reads

$$\frac{\partial \vec{c}}{\partial t} = f(\vec{c}) + D \left( \frac{\partial^2 c}{\partial x^2} + \frac{\partial^2 c}{\partial y^2} + \frac{\partial^2 c}{\partial z^2} \right) - V \left( \frac{\partial c}{\partial x} + \frac{\partial c}{\partial y} + \frac{\partial c}{\partial z} \right) \quad (8)$$

For the student, experiment Eq. (6) was used in all cases for evaluation. It was explained to the students that in all cases this evaluation represents a rough approximation. In the case of the reaction–diffusion experiments the evaluation was conducted as in the case of no reaction. Thus all students got a weakly higher diffusion coefficient. It is clear that one cannot take the term  $f(\vec{c})$  simply into the constant  $D$ . Nevertheless, such a measurement gives an indication for the propagation speed of the front. In principle

one can make some conclusions here on kinetics. Comparison to an autocatalytical reaction would be very instructive for example. For reaction–diffusion with flux no coefficients were indicated. The students should simply become acquainted with the possibility of controlling the spreading front by adjusting the flux. A detailed evaluation and discussion would blow up the possibilities within a basic course.

For comparing the diffusion coefficient of malachite green in different viscous liquid, the students had about 1.5 h for accomplishing the experiment including first part of the analysis. Twelve groups of undergraduate students could reproduce the higher diffusion coefficient in lower-viscous solutions. Comparing the results for higher and lower viscosity there was a high standard deviation in both cases, but the results were in the expected range and differed not more than one order of magnitude. The influence of the viscosity on the diffusion coefficient was evident in all experiments. Due to the Stokes–Einstein equation,  $D = kT/6\pi\eta r$ , with  $\eta$  as viscosity the diffusion coefficient was in the liquid with higher viscosity (30% glycerol) lower than in water. If we knew the viscosity of the liquid, we could calculate the hydrodynamic radius of the ions by measuring the diffusion coefficient. This was not done in our experiments, but it might be possible for future experiments.

In a second practical course 20 groups of students accomplished the experiments. These students estimated the diffusion coefficient of iron rhodanide and investigated the formation of iron rhodanide of the two educts of ammonium rhodanide and iron trichloride with and without flow. Four of the groups had well-evaluable results. That means no air bubbles in the reactor and well-defined basic conditions, like exactly measured distances and no additional artefacts in the images which are due to non-designed convection. These groups obtained a diffusion coefficient of  $D = 3.5 \times 10^{-5} \text{ cm}^2/\text{s}$  with a standard deviation of  $9.6 \times 10^{-6} \text{ cm}^2/\text{s}$  or about 28%. Considering the results of all groups the mean value of the diffusion coefficient is  $D = 2.8 \times 10^{-5} \text{ cm}^2/\text{s}$  with a standard deviation of  $2.7 \times 10^{-5} \text{ cm}^2/\text{s}$ . The experiment with in situ arising rhodanide without flow gives for all groups an averaged mean value of  $D = 6.3 \times 10^{-5} \text{ cm}^2/\text{s}$  and for the four groups with best experiments  $D = 9.4 \times 10^{-5} \text{ cm}^2/\text{s}$ , with standard deviations of  $9 \times 10^{-5}$  and  $1 \times 10^{-4} \text{ cm}^2/\text{s}$ , respectively.

## 5. Conclusion

The above described experiments were conducted in a basic course for undergraduate students. All groups obtained values in the expected range. The students could perform the experiments after short instruction autonomously. The focused teaching aim was accomplished. The students learned experimentally how the diffusion coefficient depends on viscosity and how the flow rate can be used as a parameter for influencing spatial behavior of reactants. The low-priced foil reactor was used in the same environment as real microreactors. In this way students can get the first experience of microreaction technology without using expensive microreactors.

## Acknowledgements

We thank M. Günther for discussion and ideas in designing the reactors and the Deutsche Bundesstiftung Umwelt for financial support.

## References

- [1] G. Henze, M. Köhler, J.P. Lay (Eds.), *Umweltdiagnostik mit Mikrosystemen*, Wiley, Weinheim, Germany, 1999.
- [2] P.W. Atkins, J.A. Beran, *Chemie einfach alles*, VCH, Weinheim, 1998 (Original: *General Chemistry*, 2nd ed., Freeman, New York, 1992).
- [3] P.W. Atkins, *Physical Chemistry*, 6th ed., Oxford University Press, Oxford, 1999.
- [4] W. Ehrfeld (Ed.), *Proceedings of the First (23–25 February 1997, Frankfurt/Main, Germany) and Second (8–12 March 1997, New Orleans, USA) International Conferences on Microreaction Technology*, Springer, Berlin, 1998.
- [5] J.M. Köhler, T. Mejevaia, H.P. Saluz (Eds.), *Microsystems Technology: A Powerful Tool for Biomolecular Studies*, Birkhäuser, Basel, Switzerland, 1999.
- [6] H. Reichl, A. Heuberger (Eds.), *Proceedings of the Micro System Technologies '96 (MST)*, Potsdam, Berlin, Offenbach, Germany, 17–19 September 1996, VDE-Verlag, 1996, pp. 693–698.
- [7] H. Kuhn, H.-D. Försterling, *Principles of Physical Chemistry*, Wiley, Chichester, UK, 2000.
- [8] A.F. Hollemann, N. Wiberg, *Lehrbuch der Anorganischen Chemie*, 33rd ed., Walter de Gruyter & Co, Berlin, Germany, 1985, p. 1145.
- [9] A. Bochmann, *Experimentelle Untersuchungen an biochemischen Reaktionssystemen mittels fluorimetrischer Methoden und Strömungsmechanische Simulation eines Flussreaktors*, Diploma Thesis, Friedrich-Schiller-Universität Jena, Germany, 1997.